CrystEngComm

PAPER

Three novel supramolecular hybrid compounds based on keggin polytungstates†

Li-Na Xiao,[a] **Yan Wang,**[a] **Cheng-Ling Pan,**[b] **Jia-Ning Xu,**[a] **Tie-Gang Wang,**[a] **Hong Ding,**[a] **Zhong-Min Gao,**[a] **Da-Fang Zheng,**[a] **Xiao-Bing Cui**[*a] **and Ji-Qing Xu**[*a]

Three novel supramolecular compounds $[PW^{VI}_{10.5}W^V_{1.5}O_{40}][Cu(2, 2'\text{-bpy})_2]_{4.5}$ (**1**), $[Cu^I(Phen)_2]_4[Cu^I_5Cl_4(Phen)_4][PW^{VI}_{10}W^V_2O_{40}]_2 \cdot 4H_2O(\mathbf{2})$ and $[Cu^I(Phen)_2]_4[Cu^I_5Cl_4(Phen)_4]$ $[BW^{VI}_{12}O_{40}]_2 \cdot 2H_2O(\mathbf{3})$ (bpy = bipyridine, Phen = 1,10-Phenanthroline) have been synthesized and characterized by IR, UV-Vis, TG, XRD, elemental analyses and single crystal X-ray diffraction analyses. Compound **1** is the first example of a hybrid compound which is constructed from polyoxometalates and supramolecular noncovalent coordination cages. Both compounds **2** and **3** are constructed from two different types of building blocks: polyoxometalates and metal halide fragments.

Introduction

Interest in polyoxometalates (POMs) has been continuously growing, supported by the improvement of technical structural analysis, such as X-ray diffraction and NMR, IR, and Raman spectroscopies. POMs have also received much attention because of their practical applications, due to the versatility of their properties. They have found applications in medicine, biology, catalysis, material science, *etc.*[1] The existence of POMs has already been known for almost 200 years, but the first structural details were only revealed in the last century.[2] From then on, the number of POMs developed at an exponential rate.

A recent advance in the burgeoning field of POM chemistry is the large number of hybrid compounds constructed from a combination of POMs and transition metal cations or transition metal coordination complexes (TMCs) that have been obtained. These compounds could be divided into two groups: (I) 1-D, 2-D and even 3-D extended structures through covalent interactions, for the spherical surface of POMs gives a better opportunity for forming covalent bonds with transition metal cations or TMCs.[3–6] (II) supramolecular structures constructed from POMs and TMCs through non-covalent supramolecular assembly.[7] An intelligent choice of POMs and transition metal cations or TMCs may yield materials with fascinating structures and desirable properties. The diversity of POMs and transition

metal cations or TMCs has led to a wide array of functional organic–inorganic hybrid materials.

Hybridization of redox-active inorganic clusters with transition metal coordination complexes (TMCs) could represent a versatile route to multifunctional materials that can combine the key merits of both sources, for example, magnetic, catalytic, and recognition properties.[8]

Up to now, most of the existing POM species have already been applied to act as building blocks to be connected with different TMCs into hybrids, including Keggin, Dawson POMs and so on. Previously, research into these kinds of hybrids are always focused on the choice of POMs. The TMCs are always simple with only one transition metal as the center and some organic amines as ligands.

In this article, we will report some new types of supramolecular hybrid compounds based on POMs and TMCs, of which the TMCs are not as simple as the previously reported ones. We here reported the synthesis and characterizations of a novel compound $[PW^{VI}_{10.5}W^V_{1.5}O_{40}][Cu(2, 2'\text{-bpy})_2]_{4.5}$ (**1**) which is constructed from POMs and supramolecular noncovalent coordination cages, and two novel compounds which are constructed from POMs and nona-nuclear metal halide fragments $[XW_{12}O_{40}]$ $[Cu^I_5(Phen)_4Cl_4][Cu^I(Phen)_2]_4 \cdot nH_2O$ (X = P, $n = 6$ (**2**), X = B, $n = 2$ (**3**)), the syntheses of compounds **2** and **3** provides assertive evidence for the existence of this kind of hybrid material.

Experimental

Materials and methods

All reagents were purchased commercially and used without further purification. The elemental analyses (C, H and N) were performed on a Perkin-Elmer 2400 CHN elemental analyzer. The elemental analyses (W, P and Cu) were performed on

[a]*College of Chemistry and State Key Laboratory of Inorganic Synthesis and Preparative Chemistry, Jilin University, Changchun, 130023, China. E-mail: cuixb@mail.jlu.edu.cn; xjq@mail.jlu.edu.cn*
[b]*School of Materials Science and Engineering, Anhui University of Science & Technology, Huainan, 232001, Anhui, China*

a Perkin-Elmer Optima 3300DV spectrophotometer. The infrared spectra were recorded with a Perkin-Elmer SPEC-TRUM ONE FTIR spectrometer with KBr pellets in the 4000–200cm^{-1} region. XPS measurements were performed on single crystals with ESCALAB MARK II apparatus, using the Mg–Kα (1253.6 eV) achromatic X-ray radiation source. The powder XRD patterns were obtained with a Scintag X1 powder diffractometer system using Cu–Kα radiation with a variable divergent slit and a solid-state detector. Thermogravimetric analysis (TG) data were recorded with a thermal analysis instrument (SDT 2960, TA Instruments, New Castle, DE) with the heating rate of 10 °C min^{-1} in an air flow. The UV-Vis spectra were recorded on a Shimadzu UV3100 spectrophotometer.

$[PW^{VI}_{10.5}W^{V}_{1.5}O_{40}][Cu(2, 2'\text{-bpy})_2]_{4.5}$ (1)

Compound **1** was synthesized hydrothermally by reacting of $Na_2WO_4 \cdot 2H_2O$ (0.43 g, 1.3 mmol), Sb_2O_3 (0.39 g, 1.3 mmol), 85% H_3PO_4 (0.22 g, 1.9 mmol), $CuCl_2 \cdot 2H_2O$ (0.23 g, 1.3 mmol), 2, 2'-bpy (0.16 g, 1 mmol), CH_3COOH (0.14 g, 2.3 mmol) and distilled water (15 ml) in a 25 ml Teflon-lined autoclave. The pH was adjusted to 5 with $NH_3 \cdot H_2O$ solution. The mixture was heated under autogenous pressure at 160 °C for 7 days and then left to cool to room temperature. Green crystals could be isolated in about 75% yield (based on W). Anal. Calcd for $C_{90}H_{72}Cu_{4.5}N_{18}O_{40}PW_{12}$: W, 48.29; Cu, 6.26, P, 0.68; C, 23.66; H, 1.59; N, 5.52%. Found: W, 48.13; Cu, 6.15, P, 0.53, C, 23.63; H, 1.49; N, 5.47%. IR (cm^{-1}): 1603, 1569, 1498, 1471, 1448, 1316, 1250, 1160, 1092, 1060, 1033, 999, 957, 882, 813, 728.

$[Cu^{I}(Phen)_2]_4[Cu^{I}_5Cl_4(Phen)_4][PW^{VI}_{10}W^{V}_2O_{40}]_2 \cdot 4H_2O$ (2)

Compound **2** was synthesized hydrothermally by reacting of $Na_2WO_4 \cdot 2H_2O$ (0.688 g, 2.0 mmol), KH_2PO_4 (0.278 g, 2.0 mmol), $CuCl_2 \cdot 2H_2O$ (0.397 g, 2.0 mmol), Phen $\cdot H_2O$ (0.196 g, 1.0 mmol) and distilled water (15 ml) in an 18 ml Teflon-lined autoclave. The pH of the mixture was necessarily adjusted to 5.5 with $NH_3 \cdot H_2O$ solution. The mixture was heated under autogenous pressure at 160 °C for 4 days and then left to cool to room temperature. Dark black crystals could be isolated in about 55% yield (based on W). Anal. Calcd for $C_{144}H_{104}Cl_4Cu_9N_{24}O_{44}PW_{12}$: W, 37.87; Cu, 9.82; P, 0.53; C, 29.69; H, 1.80; N, 5.77%. Found: W, 37.51; Cu, 9.83; P, 0.41; C, 29.13; H, 1.69; N, 5.37%. IR (cm^{-1}): 1622, 1574, 1505, 1422, 1136, 1100, 1062, 952, 878, 845, 790, 716, 504, 371.

$[Cu^{I}(phen)_2]_4[Cu^{I}_5Cl_4(phen)_4][BW^{VI}_{12}O_{40}]_2 \cdot 2H_2O$ (3)

The synthetic procedure of **3** was identical to **2**, but H_3BO_3 (0.129 g, 2.0 mmol) was used instead of the KH_2PO_4. The pH of the mixture was necessarily adjusted to 3 with HCl solution. The mixture was heated under autogenous pressure at 160 °C for 4 days and then left to cool to room temperature. Black crystals could be isolated in 45% yield (based on W). Anal. Calcd for $C_{144}H_{100}B_1Cl_4Cu_9N_{24}O_{42}W_{12}$: W, 38.24; Cu, 9.91; C, 29.98; H, 1.75; N, 5.83%. Found: W, 37.91; Cu, 9.83; C, 29.88; H, 1.29; N, 5.37%. IR (cm^{-1}): 1622, 1505, 1424, 1143, 990, 948, 893, 819, 721, 526, 381.

X-ray crystallography

The data for **1**, **2** and **3** were collected on a Bruker Apex II diffractometer with Mo–Kα radiation ($\lambda = 0.71073$ Å) at 293(2) K. The structures were solved by direct methods and refined by full-matrix least squares on F^2 using SHELXTL-97 software package. In the final refinements, all non-hydrogen atoms were refined anisotropically except C28 in **1**, Ow1, Ow2 and Ow3 in **2** and Ow1 in **3**. Hydrogen atoms on the 2,2'-bpy or the Phen ligands were introduced on calculated positions and included in the refinement riding on their respective parent atoms in **1**, **2** and **3**. The hydrogen atoms of 2,2'-bpy ligand coordinating to Cu2 were not added in **1**, while the hydrogen atoms on the solvent water molecules in **2** and **3** were also not added. It should be noted that positions of N5, N6, N7 and N8 in **1** are disorderly occupied by N5 and C24, N6 and C27, N7 and C31 as well as N8 and C32 with occupancy factors of 0.5, respectively. The experimental details for crystal structure determinations for **1**, **2** and **3** are listed in Table 1. CCDC number: 750860 for **1**; 777634 for **2**; 777635 for **3**.

Results and discussion

Synthesis

Parallel experiments without Sb_2O_3 for the synthesis of compound **1** have already been done, only undetermined powder was obtained. Acetic acid is also important for the preparation of **1**. Perhaps, it leads to an acetic acid–acetate buffer solution which is very important for synthesis of POMs.

The syntheses for compounds **2** and **3** are almost in a parallel experiment. The starting material molar ratios, reaction time and reaction temperature are all the same. The differences are pH values and one of the starting materials: KH_2PO_4 for **2** and H_3BO_3 for **3**, which means that the pH value is the most important factor for the final products. We only got compound **2** when the pH value was about 5.5, while when the pH value was 3, we got compound **3**. Deviations from these pH values will get either nothing, or undetermined powders. We also tried to synthesize the 2,2'-bipyridine or other halide ion analogues of compounds **2** and **3**, but unfortunately, this was still unsuccessful.

It is very interesting that the metal centers of **1**, **2** and **3** are Cu$^+$, though the starting material is $CuCl_2 \cdot 2H_2O$ with Cu^{2+} ions for all the three compounds. Actually, Cu^{2+} could be solvothermally converted into Cu$^+$ in the presence of organic species.[9]

Structure for compound 1

The examples containing both POMs and supramolecular cages are hybrid compounds based on $[V_{18}O_{42}(H_2O)]^{12-}$ and cucurbiturils.[8] The discovery of the compounds based on cucurbiturils gave us an inspiration: is it possible or not to combine the POMs with other discrete units, like the supramolecular metal ligand coordination cages, into hybrids?

In 2010, a supramolecular silver alkynyl coordination cage with sixty silver(I) ions incapsulating POMs as templates was reported by Wang *et al.*[10]

Table 1 Crystal data and structural refinements for compounds **1**, **2** and **3**

Empirical formula	$C_{90}H_{72}Cu_{4.5}N_{18}O_{40}PW_{12}$	$C_{144}H_{104}Cl_4Cu_9N_{24}O_{44}PW_{12}$	$C_{144}H_{100}BCl_4Cu_9N_{24}O_{42}W_{12}$
Formula weight	4568.76	5825.31	5769.12
Crystal system	hexagonal	Triclinic	Triclinic
Space group	$R\bar{3}c$	$P\bar{1}$	$P\bar{1}$
a (Å)	22.0053(5)	15.2200(8)	15.092(5)
b (Å)	22.0053(5)	15.9213(8)	15.819(5)
c (Å)	76.102(4)	18.079(1)	17.992(6)
α (°)	90	74.933(1)	74.792(5)
β (°)	90	74.646(1)	74.347(5)
γ (°)	120	66.294(1)	66.220(5)
Volume (Å³)	31913.9(19)	3809.2(3)	3727(2)
Z	12	1	1
D_C (Mg m⁻³)	2.853	2.539	2.570
μ (mm⁻¹)	13.899	10.411	10.627
$F(000)$	25098	2719	2689
θ for data collection	1.20 to 26.06	1.19 to 26.14	1.74 to 26.42
Reflections collected	57331	21397	20712
Reflections unique	7040	14992	14944
R_{int}	0.0634	0.0265	0.0744
Completeness to θ (%)	100%	98.7	97.7
Data/parameters	7040/1/498	14992/1087	14944/1079
GOF on F^2	1.188	1.042	1.030
$R_1{}^a$ [$I > 2\sigma(I)$]	0.0482	0.0512	0.01053
w$R_2{}^b$ (all data)	0.1411	0.1609	0.2807

^{a} R$_1 = \sum\|$F$_0| - |$F$_c\|/\sum|$F$_0|$. ^{b} ωR$_2 = \{\sum[$w (F$_0^2$ − F$_c^2$)^2]/$\sum[$w(F$_0^2$)^2]\}^{1/2}$.

Also in 2010, Jansen *et al.* reported a novel compound which contains POMs [CoW$_{12}$O$_{40}$]$^{6-}$ and [Ag$_{42}$] supramolecular cages.[11] In 2007 and 2010, Lu *et al.* reported several compounds [Ag$_6$(3atrz)$_6$][PMo$_{12}$O$_{40}$]$_2$·H$_2$O, [Cu$_6$(4atrz)$_6$][PMo$_{12}$O$_{40}$]$_2$·H$_2$O and [Cu$_4$(4atrz)$_6$][SiW$_{12}$O$_{40}$] (3atrz = 3-amino-1,2,4-triazole, 4atrz = 4-amino-1,2,4-triazole), each of which contains POMs and supramolecular cages.[12] Lu *et al.* also reported another compound in 2010, constructed from complex Ag$_{24}$ cages and POMs.[13]

Comparing the compounds reported by Wang, Jansen and Lu *et al.* in detail, we found that these compounds can be grouped as one type of supramolecular hybrids which are constructed from POMs and supramolecular metal ligand coordination cages. This type of hybrid can be divided into two subgroups: the first is exemplified by the compound synthesized by Wang *et al.* The capacity of the supramolecular cage of the first type is big enough, and the body of the POM of the first type is small, so the supramolecular cage can encapsulate the POM (as shown in Fig. 1(a)). The second type is exemplified by the compounds by Lu and Jansen *et al.* The capacity of the supramolecular cage and the body of the POM of this type are comparable, so the supramolecular cage can not encapsulate the POM, thus, the

POMs are located outside the supramolecular cages and exist together with the supramolecular cages into hybrids (as shown in Fig. 1(b)).

Wang, Jansen and Lu *et al.* only described those compounds as "inorganic–organic hybrids", however, here we think these compounds could be classified as the first examples of compounds based on POMs and supramolecular coordination cages.

By analysing the compounds by Wang, Jansen and Lu *et al.* in detail, we found that all the supramolecular coordination cages of the compounds are assembled through covalent interactions. However, there is another kind of supramolecular cage structure constructed from transition metal coordination fragments assembled through non-covalent interactions.[14] To the best of our knowledge, hybrids based on POMs and supramolecular noncovalent coordination cages have not yet been reported.

Here we reported the structure of compound **1**, which is the first example constructed from POMs and supramolecular non-covalent coordination cages. The crystal structure of **1** shows striking complementarity between the polyoxometalatic and supramolecular entities, as seen in Fig. 2. [PW$^{VI}_{10.5}$W$^V_{1.5}$O$_{40}$]$^{4.5-}$ may be viewed as a shell of {W$_{12}$O$_{36}$} encapsulating a PO$_4$ moiety, present at its centre and responsible for the local tetrahedral geometry. Each oxygen atom of the PO$_4$ group, bonded to three different tungsten centers of the shell, is in a bridging mode with P–O distances in the 1.529(15)–1.539(9) Å range. According to different coordination environments, oxygen atoms can be divided into three groups: W–O$_t$, W–O$_b$ and W–O$_c$ bonds, with bond distances falling in the ranges of 1.696(9)–1.709(8), 1.866(8)–1.949(8) and 2.421(9)–2.453(8) Å, respectively. Oxidation states for W atoms were calculated using parameters given by Brown.[15] Results give the average value 5.875 for tungsten atoms, which reveals that the oxidation state of 10.5 tungsten atoms is +6 and the remaining 1.5 tungsten atoms is +5. Thus the formula of the POM is [PW$^{VI}_{10.5}$W$^V_{1.5}$O$_{40}$]$^{4.5-}$.
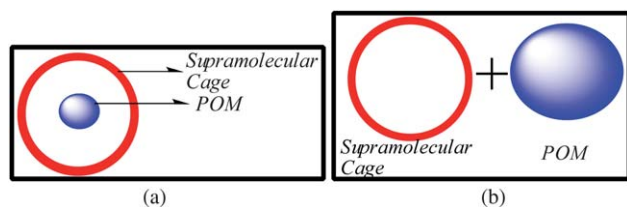
Fig. 1 (a) Schematic representation of the first type of hybrids based on POMs and supramolecular coordination cages; (b) Schematic representation of the second type of hybrids based on POMs and supramolecular coordination cages.
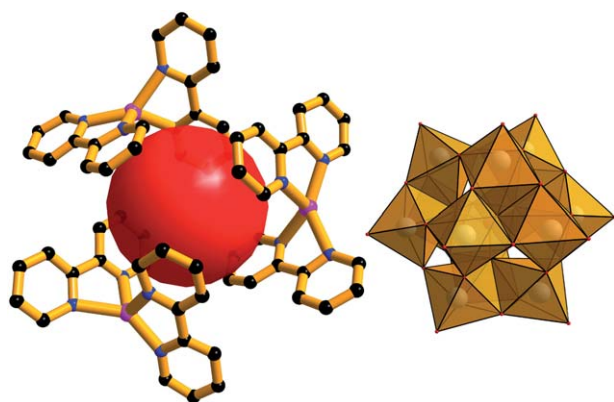
Fig. 2 The ball-and-stick and polyhedron representation of the combination of the supramolecular triangle and the Keggin anion in **1**. The big ball represents the internal volume of the cage.

Three $[Cu2(2,2'-bpy)_2]^+$ transition metal coordination fragments (TMCs) interact with each other through non-covalent interactions into a novel supramolecular cage, as shown in Fig. 2. It should be noted that the supramolecular coordination cage of focus is the simplest one, compared with other reported supramolecular coordination cages. The three metal centers of the TMCs are arranged into an equilateral triangle motif with metal–metal distances of any two of the three TMCs of 8.5116(1) Å. The pyridyl rings of ligands wrap "over and under" the plane formed by the three metal ions, leading to a trinuclear, triangular, circular cage with cage diameter about 7.63 Å. The pyridyl rings of the TMCs create an inner core. There is a significant space within this inner core estimated at about 230 Å^3.

As shown in Fig. 2, the Cu2 is coordinated by two 2,2′-bpy ligands, which is bonded to N5 and N6 from one 2,2′-bpy (**L1**), as well as N7 and N8 from the other 2,2′-bpy (**L2**). The dihedral angles of the two pyridyl rings of **L1** and **L2** are 9.396°, indicating that the pyridyl rings of **L1** and **L2** are almost coplanar, respectively. The dihedral angle between the plane through Cu2, N5 and N6 (**plane 1**) and the plane through Cu2, N7 and N8 (**plane 2**) is 86.209°. The dihedral angles between **plane 1** and the two pyridyl rings of **L1** range from 21.999–22.377°, indicating that **plane 1** is not coplanar with the plane formed by the pyridyl rings of **L1**, while dihedral angles between **plane 2** and the two pyridyl rings of **L2** range from 42.782–43.639°, which obviously show that the **plane 2** could not be coplanar with the plane formed by pyridyl rings of **L2**. The **plane 2** and the plane formed by pyridyl rings of **L2** exhibit a novel V-shaped conformation. To the best of our knowledge, it is the first time that such a novel coordination mode has been observed. It is thought that this novel coordination mode of Cu2 leads to the novel supramolecular cage in **1**.

Detailed analysis of the supramolecular cage reveals that there exists no hydrogen bonding or π⋯π interactions between any two of the three Cu2 TMCs. Such an interesting arrangement perhaps comes from the synergism interactions of the TMCs and the POMs.

Several supramolecular triangles have already been reported,[16,17] all those triangles are constructed from three metal ions with ligands as bridges through covalent linking. However, the triangle in **1** is constructed from three discrete TMCs, no ligand

links any two of the three Cu ions. To the best of our knowledge, it is the first supramolecular triangle connected through non-covalent interactions.

The packing motif of supramolecular cages and POMs is interesting. Each cage is involved with 6 neighbouring POMs through 6 C–H⋯O hydrogen bonding interactions, while each POM also interacts with 3 cages with C–H⋯O hydrogen bonding interactions. The C⋯O distances are 3.2292(1) Å. Fig. 3 shows how these C–H⋯O interactions collectively help to construct a large infinite 2-D layer structure along the crystallographic *ab* plane.

There also exists a common pseudo-tetrahedral coordination $[Cu1(2,2'-bpy)_2]^+$ TMC in **1** which serve as counterions. **1** is constructed from POMs and $[Cu(2,2'-bpy)_2]^+$ units, which contain a great deal of pyridyl rings. However, there exists no π⋯π stacking interaction in **1**, which has been confirmed by the Platon software.[18] The lack of π⋯π stacking interactions could perhaps be attributed to the steric hindrance of POMs.

The preparation of **1** represents the discovery of a new type of hybrid materials constructed from POMs and supramolecular cages. **1** is the first example of this type of hybrid material; it opens a new gateway in POM or supramolecular chemistry.

The unique structural feature of **1** suggests that the current discovery is just a tip of the iceberg and this new type of compound may be a prevalent one in the world of POM or supramolecular chemistry. If a supramolecular cage with larger volume was introduced into the system of POM, it will significantly influence the properties of hybrid products such as catalysis, material science, medicine, and so on.

Structures for compound 2 and 3

The POM compounds containing halide ions have been reported for years by several research groups.[1,19–21] The roles of the halide ions in POM compounds could be divided into three types: (I) halide ions act as templates with no covalent interactions with any metal atoms. Müller *et al.* and Khan *et al.* reported a series of
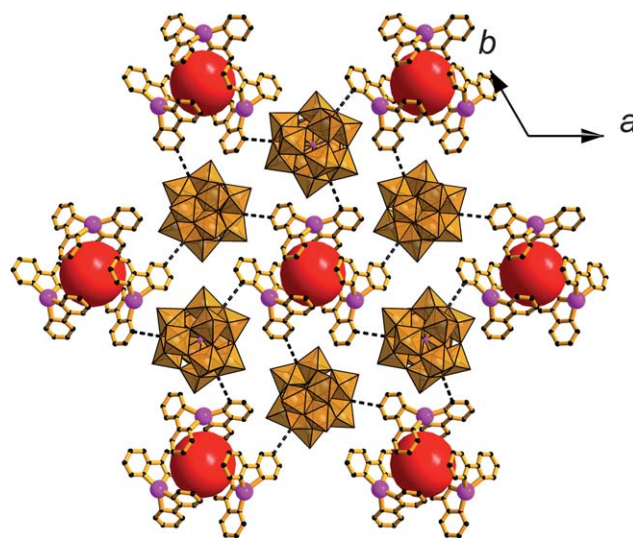
Fig. 3 The 2-D layer structure constructed from supramolecular cages and POMs through C–H⋯O hydrogen bonding interactions.

$V_{18}O_{42}$ POMs encapsulating halide ions.[19] In 2005 and then in 2009, Kortz *et al.* reported several $[Cu_{20}X(OH)_{24}(H_2O)_{12}(P_8W_{48}O_{184})]^{25-}$ (X = Cl, Br, I) ions, with halide ions included at the centre of the POMs.[20] The halide ions in these reported POM compounds only serve as templates. (II) Halide ions serve as terminal monodentate ligands. This kind of POM compounds containing halide ions is exemplified by compound $[Cu^I_3Cl(4,4'-bipy)_4][Cu^{II}(1,10-phen)_2Mo_8O_{26}]$, reported by Wang *et al.*,[21] which contains halide ions as terminal monodentate ligands coordinating to copper ions. Only a few compounds could be grouped as type I and type II.

In contrast to type I and type II, there exists type III, of which halide ions act as multidentate ligands. This type is more interesting and important, for multidentate halide ions with metal atoms will yield metal halide fragments.

To the best of our knowledge, a variety of metal halide fragments were reported,[22] as well as a large number of POMs,[1] thus the number of hybrids (type III) based on the combination of POMs and metal halide fragments should be large. However, after searching the literature, we found only the compound $[Cu_2(2,2'-bpy)_4Cl][Cu(2,2'-bpy)_2SeW_{12}O_{40}]\cdot 2H_2O$, reported by Niu *et al.*,[23] which was not thought as "novel" at the time.

The compound reported by Niu *et al.* could just be regarded as the first hybrid compound (type III) constructed from two building blocks: POMs and metal halide fragments, though the metal halide fragment is the simplest one which contains only one multidentate chloride ion and two metal atoms. In contrast, the ones by Müller, Khan, Kortz or Wang could not be regarded as being constructed from POMs and metal halide fragments, the halide ions of which either are included in the POMs or coordinate to the metal centers as terminal ligands.

It is almost impossible for anyone to judge whether the compound $[Cu_2(2,2'-bpy)_4Cl][Cu(2,2'-bpy)_2SeW_{12}O_{40}]\cdot 2H_2O$ is a special case or not. If not, the discovery will be a tip of the iceberg. As is well known, the variety of metal halide fragments and POMs will lead to a large number of hybrids. Alternatively, the metal halide fragments of the compound by Niu *et al.* is too simple and "alone" to demonstrate that there exists a new kind of hybrid based on POMs and metal halide fragments. Thus, we must find other compounds constructed from POMs and complex metal halide fragments, and only these will provide assertive evidence for the existence of this new type of hybrid material. Here we reported the structures of compounds **2** and **3**, which are just the compounds constructed from POMs and complex metal halide fragments we wanted.

The POMs of focus are Keggin archetype, $\{XW_{12}O_{40}\}$ (X = P, B). Syntheses of the two hybrid complexes of $\{XW_{12}\}$ (X = P, B) and metal halide fragments were accomplished by the hydrothermal method. The compounds $[XW_{12}O_{40}][Cu^I_5(Phen)_4Cl_4][Cu^I(Phen)_2]_4\cdot nH_2O$ (X = P, n = 4 (**2**), X = B, n = 2 (**3**)) were isolated as black crystals. The preparations for **2** and **3** demonstrated the existence of a new type of hybrid material based on POMs and metal halide fragments. Single crystal X-ray diffraction analyses reveal that **2** and **3** are isomorphous; compound **2** is described in detail below as an example.

$[PW_{12}O_{40}]^{5-}$ may be viewed as a shell of $\{W_{12}O_{36}\}$ encapsulating a PO_4 moiety, in which the P1 atom lies on an inversion centre and is bonded to eight half-occupancy oxygen atoms with P–O distances of 1.454(13)–1.561(15) Å. According to different coordination environments, oxygen atoms can be divided into three groups: W–O$_t$, W–O$_b$ and W–O$_c$, with bond distances in the ranges of 1.673(8)–1.736(11), 1.871(10)–1.925(9) and 2.402(14)–2.463(13) Å, respectively. Oxidation states for W atoms were calculated using parameters given by Brown.[15] Results reveal that oxidation states of 10 tungsten atoms are +6 and 2 tungsten atoms are +5. Thus the formula of the POM is $[PW^{VI}_{10}W^V_2O_{40}]^{5-}$.

There are two different units, except for the anion $[PW_{12}O_{40}]^{5-}$, metal halide fragments $[Cu^I_5(Phen)_4Cl_4]^+$ and transition metal coordination fragments (TMCs) $[Cu^I(Phen)_2]^+$. The first is a novel nona-nuclear metal halide fragments consisting of five copper(I) ions, four chloride ions and four Phen ligands. As shown in Fig. 4, the Cu5, exhibiting a trigonal coordination environment, receives contributions from two nitrogen donors from one Phen, with distances of 2.013(11)–2.061(12) Å, and one chloride donor Cl1 with a distance of 2.123(4) Å. The Cu4, exhibiting a distorted tetrahedral coordination environment, receives contributions from two nitrogen donors from one Phen ligand with distances of 1.982(14)–2.125(19) Å, and two chloride donors of Cl1 and Cl2 with distances of 2.876(5) Å and 2.237(5) Å. The Cu5 and Cu4 are connected through the linking of the Cl1 ion. In contrast to Cu5 and Cu4, the Cu3 is coordinated by only two Cl2 ions with a distance of 2.138(4) Å, exhibiting a linear coordination environment. The Cu4 and Cu3 are joined by the linking of the Cl2 ion. Thus two Cu5, two Cu4 and one Cu3 are connected together by two Cl1 and two Cl2 into a novel nona-nuclear metal halide fragments. It should be noted that the Cu3 lies on an independent inversion centre, which is also the inversion center of the fragment, and only Cu3 is not coordinated by the Phen ligands, owing to the steric hindrance.

Alternatively, there are three types of copper coordination environments in the nona-nuclear metal halide fragment: two trigonal, two tetrahedral and one linear coordination
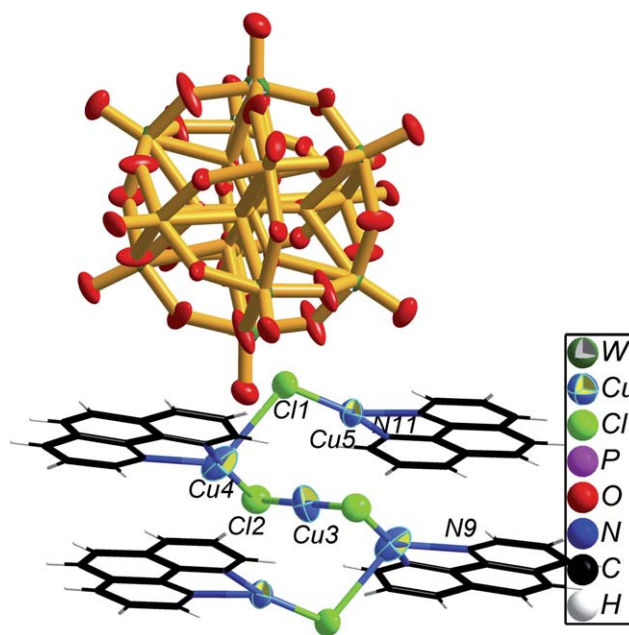
Fig. 4 The representation of the metal halide cluster $[Cu^I_5(Phen)_4Cl_4]^+$ and the $[PW_{12}O_{40}]^{5-}$.

environment. To the best of our knowledge, such a discrete metal halide nona-nuclear fragment has never been reported before. In addition, another interesting feature is that there are intra-molecular $\pi\cdots\pi$ interactions between the N9 and N11 Phen ligands. These two Phen ligands are arranged parallel with each other, the distance between the N9 and N11 Phen ligands is about 3.41–3.46 Å.

The transition metal coordination fragment $[Cu^I(Phen)_2]^+$ exhibits a tetrahedral coordination environment with copper centres coordinated by four nitrogen donors from two Phen ligands, with distances of 1.992(11)–2.065(10) Å. It should be noted that there are two such TMCs with a Cu1–Cu2 distance of 3.936(3) Å. The N1 Phen of the Cu1 TMC is arranged parallel with the N5 Phen of the Cu2 TMC, while the N3 Phen of the Cu1 TMC is arranged parallel with the N7 Phen of the Cu2 TMC. The interplanar distances of N1 to N5 ligands and N3 to N7 ligands are about 3.45 Å, which means strong inter-molecular $\pi\cdots\pi$ interactions. It should be noted that the phenol rings of the N1, N3 Phen could not fully overlap those of the N5, N7 Phen, which means that only parts of the phenol rings of N1, N3 Phen overlap those of N5, N7 Phen. However, the distance of these phenol rings means very strong $\pi–\pi$ interactions by partly overlapping. Alternatively, a novel supramolecular dimer was constructed from two $[Cu^I(Phen)_2]^+$ TMCs through strong $\pi\cdots\pi$ interactions. Oxidation states for all the Cu atoms were calculated.[24] The results reveal that the oxidation states of all the copper atoms are +1.

An unusual feature of 1 is the stacking fashion of the nona-nuclear fragments $[Cu^I_5(Phen)_4Cl_4]^+$ and the supramolecular dimers. As shown in Fig. 5, there are two supramolecular dimers between every two $[Cu^I_5(Phen)_4Cl_4]^+$, the "left" dimer interacts with the "upper" and the "lower" $[Cu^I_5(Phen)_4Cl_4]^+$ through strong inter-molecular $\pi\cdots\pi$ interactions between the N3, N7 Phen of the dimer and the N9, N11 Phen of the metal halide fragments with interplanar distances of about 3.45 Å, while the "right" dimer shows the similar $\pi\cdots\pi$ interactions with the "upper" and the "lower" metal halide fragments with similar interplanar distances of about 3.45 Å. Thus, the fragments $[Cu^I_5(Phen)_4Cl_4]^+$ and the supramolecular dimers stacked into a novel supramolecular infinite straight column structure along a axis. Such a supramolecular straight column structure has never been reported before.

Another unusual feature is the 2-D supramolecular layer stacked by the supramolecular infinite columns constructed from metal halide fragments and the supramolecular dimers. As shown in Fig. 6, the N3 and N7 Phen of the supramolecular dimer are parts of the supramolecular column, while the N1 and N5 Phen of the supramolecular dimer are exerted out of the supramolecular column. The exerted Phen ligands from two adjacent supramolecular columns interact with each other through strong inter-molecular $\pi\cdots\pi$ interactions between two N1 Phen of two supramolecular dimers from adjacent supra-molecular columns, with interplanar distances of about 3.45 Å. Alternatively, the inter-molecular $\pi\cdots\pi$ interactions of the supramolecular dimers join the adjacent supramolecular columns into a novel supramolecular layer structure along the b axis, constructing a novel supramolecular layer structure.

The most unusual feature of 1 is the combination of the supramolecular layer constructed by the supramolecular
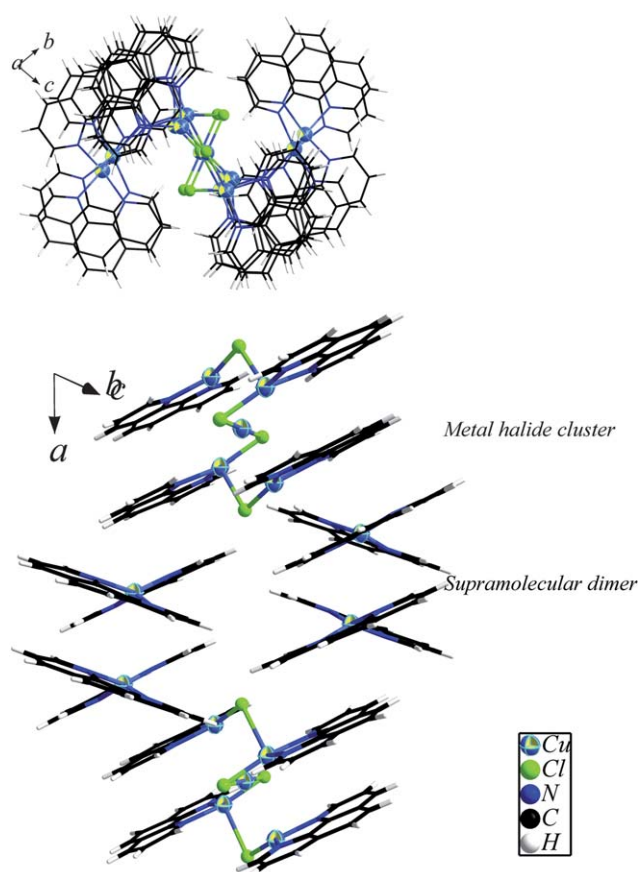
Fig. 5 (a) The upper view of the representation of the supramolecular infinite straight column structure along the a axis constructed from metal halide clusters and supramolecular dimers. (b) The side view of the supramolecular column.

columns with the $[PW_{12}O_{40}]^{5-}$ polyoxometalates, as shown in Fig. 7. Discrete POMs are sandwiched by two infinite layers, while each layer is decorated by POMs, above and below. It should be noted that the centroid–centroid distance of the POMs is 15.92(2) Å along the b axis and 15.22(2) Å along the a axis.

The detailed analysis shows that POMs exhibit extensive hydrogen-bonding interactions between oxygen atoms of POMs and carbon atoms of Phen ligands in supramolecular layers (Table s1, ESI†). Thus, complex hydrogen bonds between POMs and supramolecular layers connect the two different parts, which means that hydrogen bonds connect adjacent POMs and
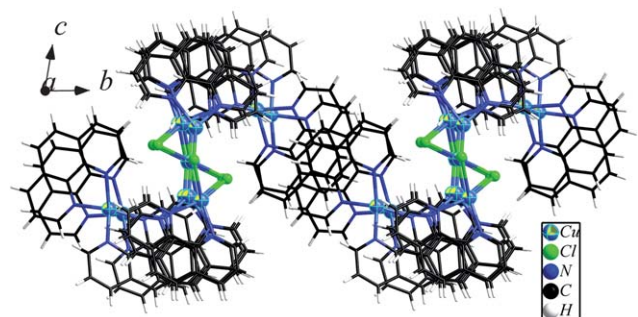
Fig. 6 The side-view of the supramolecular layer.
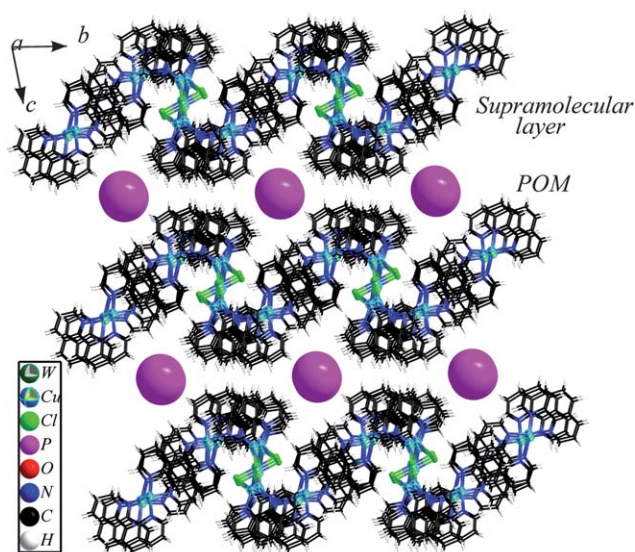
Fig. 7 The representation of the hybrid constructed from POMs and metal halide clusters. The big ball represents the POM.

supramolecular layers into a novel 3-D supramolecular structure, as shown in Fig. 7.

XPS analyses

The tungsten oxidation state calculated from bond valence sum calculations was confirmed by the XPS spectrum for **1** (fig. s1, ESI†), which gives four overlapped peaks at 38.6 eV, 37.2 eV, 35.8 eV and 35.0 eV, attributed to W^{6+} 4f5/2, W^{5+} 4f5/2, W^{6+} 4f7/2 and W^{5+} 4f7/2, respectively, being ascribed to the mixture of W^{5+} and W^{6+}.

The oxidation states for tungsten atoms of **2** are further confirmed by the XPS analysis. The XPS spectrum for **2** presents four overlapped peaks at 38.6 eV, 37.2 eV, 36.1 eV and 35.0 eV, attributed to W^{6+} 4f5/2, W^{5+} 4f5/2, W^{6+} 4f7/2 and W^{5+} 4f7/2, respectively, which should be ascribed to the mixture of W^{5+} and W^{6+} (as shown in Fig. s2, ESI†).

The XPS spectrum for **3** exhibits two peaks at 37.1 eV and 35.2 eV, attributed to W^{6+} 4f5/2 and W^{6+} 4f7/2, respectively, which should be ascribed to the W^{6+} (as shown in Fig. s2, ESI†). The XPS estimation of the valence is in reasonable agreement with those calculated from bond valence sum calculations.

UV-Vis spectrum

The UV-Vis spectrum for compound **1**, in the range of 260–450nm, are presented in Fig. s3, ESI.† The UV-Vis spectrum of compound **1** displays a wide medium intense absorption peak at about 280 nm and a shoulder peak at 314 nm, assigned to O→W charge transfer in the polyoxoanion structure.

The UV-Vis spectra for compound **2–3**, in the range of 250–800 nm, are presented in Fig. s4, ESI.† The UV-Vis spectrum for compound **2** consists of two well separated bands at about 271 nm and 445 nm assigned to O→W charge transfer and π→π* transitions in the polyoxoanion structure of **2**. The UV-Vis spectrum for compound **3** exhibits similar absorption peaks at 271 nm and 445 nm, attributed to charge transfer bands of

O→W and π→π* transitions in the polyoxoanion structure of **3**. The UV-Visible absorption spectra are very similar, indicating that compounds **2** and **3** are isomorphous.

XRD analyses

The powder X-ray diffraction pattern for **1** at room temperature is in good agreement with the one simulated based on the data of the single-crystal structure (fig. s5, ESI†), indicating the purity of the synthesized product. The differences in reflection intensity are probably due to preferred orientations in the powder samples of compound **1**. The XRD behavior for compound **1** after 2 h heat treatment at 200 °C was also investigated and is also in good agreement with the simulated one (fig. s5, ESI†), indicating that compound **1** is stable even at high temperatures.

The powder X-ray diffraction patterns for **2** and **3** are in good agreement with the ones simulated based on the data of the single-crystal structures (as shown in Fig. s6, ESI†), indicating the purity of the synthesized products. The differences in reflection intensity are probably due to preferred orientations in the powder samples of compound **2** and **3**.

IR spectrum for 2 and 3

The compositional analyses for **2** and **3** were not only carried out by elemental analyses, but can also be confirmed by the IR analyses. The IR spectra for **2** and **3** are similar (as shown in Fig. s7, ESI†). However, there is a significant difference between the IR spectra for **2** and **3**. There is a strong absorption band at 1062 cm^{-1} in the spectrum for **2** but not in the spectrum for **3**, which could be attributed to the P–O stretching vibration, indicating that the central atom of **2** is P.

TG analyses

The TG analysis for compound **1** has been done from 30 to 800 °C. The TG analysis reveals that compound **1** is stable until 310 °C. From 310 °C to 780 °C, the TG curve (Fig. s8, ESI†) exhibits a continuous decrease with a weight loss of 30.2%, being consistent with the release of the bpy ligands (Calcd: 30.8%).

The crystal analyses and elemental analyses for both **2** and **3** can be further confirmed by the TG analyses for **2** and **3**. The TG analyses for **2** and **3** (as shown in Fig. s9, ESI†) have been carried out. The TG curve exhibits a continuous decrease from 40–676 °C with a weight loss of 41.95% for **2**, corresponding to the release of the water molecules, the chloride ions and the Phen ligands (calculated: 40.79%), while the TG curve for **3** exhibits a continuous decrease from 40–629 °C with weight loss of 40.63%, corresponding to the release of the water molecules, the chloride ions and the Phen ligands (calculated: 40.57%).

Conclusions

The preparation of **1** represents the first example of a new type of hybrid material constructed from POMs and noncovalent supramolecular cages. Compounds **2** and **3** are just the assertive evidence for the existence of another new type of hybrids based on POMs and metal halide fragments. **1** opens a new gateway in POM or supramolecular chemistry. **2** and **3** present a new interdiscipline of polyoxometalate and metal halide fragments.

Acknowledgements

Notes and references

1 (a) M. T. Pope, *Heteropoly and Isopoly Oxometalates*, Springer-Verlag, Berlin, 1983; (b) M. T. Pope and A. Müller, *Angew. Chem., Int. Ed. Engl.*, 1991, **30**, 34; (c) M. T. Pope, A. Müller, *Polyoxometalates: From Platonic Solids to Anti-Retro Viral Activity*, Kluwer, Dordrecht, The Netherlands, 1994; (d) C. Hill, *Polyoxometalates, Chem. Rev.*, 1998, **98**; (e) M. T. Pope, A. Müller, *Polyoxometalate Chemistry: From Topology* via *Self-Assembly to Applications*, Kluwer, Dordrecht, the Netherlands, 2001; (f) T. Yamase, M. T. Pope, *Polyoxometalate Chemistry for Nano-Composite Design*, Kluwer, Dordrecht, the Netherlands, 2002.

2 (a) J. F. Keggin, *Nature*, 1933, **131**, 908; (b) J. Berzelius, *Ann. Phys. Chem.*, 1826, **6**, 369.

3 (a) M. I. Khan, E. Yohannes and R. J. Doedens, *Angew. Chem., Int. Ed.*, 1999, **38**, 1292; (b) J. Lu, Y. Xu, N. K. Goh and L. S. Chia, *Chem. Commun.*, 1998, 2733–2734; (c) A. Tripathi, T. Hughbanks and A. Clearfield, *J. Am. Chem. Soc.*, 2003, **125**, 10528; (d) J. R. D. Debord, R. C. Haushalter, L. M. Meyer, D. J. Rose, P. J. Zapf and J. Zubieta, *Inorg. Chim. Acta*, 1997, **256**, 165; (e) P. J. Hagrman, D. Hagrman and J. Zubieta, *Angew. Chem., Int. Ed.*, 1999, **38**, 2638; (f) D. Hagrman, C. Zubieta, D. J. Rose, J. Zubieta and R. C. Haushalter, *Angew. Chem., Int. Ed. Engl.*, 1997, **36**, 873; (g) A. Dolbecq, P. Mialane, L. Lisnard, J. Marrot and F. Sécheresse, *Chem.–Eur. J.*, 2003, **9**, 2914; (h) P. Mialane, A. Dolbecq and F. Sécheresse, *Chem. Commun.*, 2006, 3477; (i) S. Reinoso, P. Vitoria, J. M. Gutiérrez-Zorrilla, L. Lezama, L. San Felices and J. I. Beitia, *Inorg. Chem.*, 2005, **44**, 9731; (j) J. Thomas and A. Ramanan, *Cryst. Growth Des.*, 2008, **8**, 3391; (k) K. Pavani, S. E. Lofland, K. V. Ramanujachary and A. Ramanan, *Eur. J. Inorg. Chem.*, 2007, 568.

4 (a) C. Lei, J.-G. Mao, Y.-Q. Sun and J.-L. Song, *Inorg. Chem.*, 2004, **43**, 1964; (b) C. Liu, D. Zhang, M. Xiong and D. Zhu, *Chem. Commun.*, 2002, 1416; (c) Y.-P. Ren, X.-J. Kong, X.-Y. Hu, M. Sun, L.-S. Long, R.-B. Huang and L.-S. Zheng, *Inorg. Chem.*, 2006, **45**, 4016; (d) G.-C. Qu, L. Jiang, X.-L. Feng and T.-B. Lu, *Dalton Trans.*, 2009, 71; (e) J.-Y. Niu, D.-J. Guo, J.-P. Wang and J.-W. Zhao, *Cryst. Growth Des.*, 2004, **4**, 241; (f) S.-T. Zheng, J. Zhang and G.-Y. Yang, *Angew. Chem., Int. Ed.*, 2008, **47**, 3909; (g) J.-W. Zhao, C.-M. Wang, J. Zhang, S.-T. Zheng and G.-Y. Yang, *Chem.–Eur. J.*, 2008, **14**, 9223; B.-Z. Lin and S.-X. Liu, *Chem. Commun.*, 2002, 2126.

5 (a) X.-B. Cui, J.-Q. Xu, H. Meng, S.-T. Zheng and G.-Y. Yang, *Inorg. Chem.*, 2004, **43**, 8005; (b) C. Pan, J. Xu, G. Li, X. Cui, L. Ye and G. Yang, *Dalton Trans.*, 2003, 517; (c) X.-B. Cui, J.-Q. Xu, Y. Li, Y.-H. Sun and G.-Y. Yang, *Eur. J. Inorg. Chem.*, 2004, 1051; (d) L.-J. Zhang, X.-L. Zhao, J.-Q. Xu and T.-G. Wang, *J. Chem. Soc., Dalton Trans.*, 2002, 3275; (e) S.-Y. Shi, Y. Chen, J.-N. Xu, Y. Wang, G.-W. Wang, X.-B. Cui, G.-D. Yang and J.-Q. Xu, *Dalton Trans.*, 2010, **39**, 1389; (f) S.-Y. Shi, Y.-C. Zou, X.-B. Cui, J.-N. Xu, Y. Wang, G.-W. Wang, G.-D. Yang and J.-Q. Xu, *CrystEngComm*, 2010, **12**, 2122; (g) S.-Y. Shi, Y. Chen, J.-N. Xu, Y.-C. Zou, X.-B. Cui, Y. Wang, T.-G. Wang, J.-Q. Xu and Z.-M. Gao, *CrystEngComm*, 2010, **12**, 1949; (h) Y. Wang, L. Ye, T.-G. Wang, X.-B. Cui, S.-Y. Shi, G.-W. Wang and J.-Q. Xu, *Dalton Trans.*, 2010, **39**, 1916.

6 (a) H.-Y. An, Y.-G. Li, E.-B. Wang, D.-R. Xiao, C.-Y. Sun and L. Xu, *Inorg. Chem.*, 2005, **44**, 6062; (b) H.-Y. An, E.-B. Wang, D.-R. Xiao, Y.-G. Li, Z.-M. Su and L. Xu, *Angew. Chem., Int. Ed.*, 2006, **45**, 904; (c) J. Lü, E.-H. Shen, Y.-G. Li, D.-R. Xiao, E.-B. Wang and L. Xu, *Cryst. Growth Des.*, 2005, **5**, 65; (d) C.-Y. Sun, Y.-G. Li, E.-B. Wang, D.-R. Xiao, H.-Y. An and L. Xu, *Inorg. Chem.*, 2007, **46**, 1541; (e) Y. Lu, Y. Xu, E.-B. Wang, X.-X. Xu and Y. Ma, *Inorg. Chem.*, 2006, **45**, 2055; (f) H.-Y. An, Y.-G. Li, D.-R. Xiao, E.-B. Wang and C.-Y. Sun, *Cryst. Growth Des.*, 2006, **6**, 1107.

7 (a) P. Q. Zheng, Y. P. Ren, L. S. Long, R. B. Huang and L. S. Zheng, *Inorg. Chem.*, 2005, **44**, 1190; (b) X. L. Wang, C. Qin, E. B. Wang, Y. G. Li, N. Hao, C. W. Hu and L. Xu, *Inorg. Chem.*, 2004, **43**, 1850; (c) C. P. Pradeep, D. L. Long, G. N. Newton, Y. F. Song and L. Cronin, *Angew. Chem., Int. Ed.*, 2008, **47**, 4388; (d) Z. H. Yi, X. B. Cui, X. Zhang, G. D. Yang, J. Q. Xu, X. Y. Yu, H.-H. Yu and W. J. Duan, *J. Mol. Struct.*, 2008, **891**, 123; (e) T. R. Veltman, A. K. Stover, A. N. Sarjeant, K. M. Ok, P. S. Halasyamani and A. J. Norquist, *Inorg. Chem.*, 2006, **45**, 5529; (f) R. Atencio, A. Briéno and X. Galindo, *Chem. Commun.*, 2005, 637; (g) R. Atencio, A. Briceño, P. Silva, J. A. Rodríguez and J. C. Hanson, *New J. Chem.*, 2007, **31**, 33; (h) Y. Wang, C. L. Pan, L. N. Xiao, F. Q. Wu, H. Ding, Y. B. Liu, Z. M. Gao, D. F. Zheng, T. G. Wang, G. D. Yang, X. B. Cui and J. Q. Xu, *J. Solid State Chem.*, 2010, **183**, 2862.

8 X. K. Fang, P. Kögerler, L. Isaacs, S. Uchida and N. Mizuno, *J. Am. Chem. Soc.*, 2009, **131**, 432.

9 X. M. Chen and M. L. Tong, *Acc. Chem. Res.*, 2007, **40**, 162.

10 J. Qiao, K. Shi and Q. M. Wang, *Angew. Chem., Int. Ed.*, 2010, **49**, 1765.

11 F. Gruber and M. Jansen, *Angew. Chem., Int. Ed.*, 2010, **49**, 4924.

12 (a) Q. G. Zhai, X. Y. Wu, S. M. Chen, Z. G. Zhao and C. Z. Lu, *Inorg. Chem.*, 2007, **46**, 5046; (b) X. Y. Wu, X. F. Kuang, Z. G. Zhao, S. C. Chen, Y. M. Xie, R. M. Yu and C. Z. Lu, *Inorg. Chim. Acta*, 2010, **363**, 1236.

13 X. F. Kuang, X. Y. Wu, R. M. Yu, J. P. Donahue, J. S. Huang and C. Z. Lu, *Nat. Chem.*, 2010, **2**, 461.

14 L. J. Childs, N. W. Alcock and M. J. Hannon, *Angew. Chem., Int. Ed.*, 2001, **40**, 1079.

15 I. D. Brown, in *Structure and Bonding in Crystals* (ed.: M. O'Keefe, A. Navrotsky), Academic Press, New York, 1981, vol. 2, pp. 1–30.

16 (a) R. D. Schnebeck, E. Freisinger and B. Lippert, *Chem. Commun.*, 1999, 675; (b) M. C. Jennings and R. J. Puddephatt, *Chem. Commun.*, 2001, 2676; (c) I. M. Müller, R. Robson and F. Separovic, *Angew. Chem., Int. Ed.*, 2001, **40**, 4385.

17 L. J. Childs, N. W. Alcock and M. J. Hannon, *Angew. Chem., Int. Ed.*, 2002, **41**, 4244.

18 A. L. Spek, *PLATON, a multipurpose crystallographic tool*, Utrecht University, Utrecht, The Netherlands, 2001.

19 (a) A. Müller, R. Sessoli, E. Krickemeyer, H. Bögge, J. Meyer, D. Gatteschi, L. Pardi, J. Westphal, K. Hovemeier, R. Rolhfing, J. Döring, F. Hellweg, C. Beugholt and M. Schmidtmann, *Inorg. Chem.*, 1997, **36**, 5239; (b) M. I. Khan, E. Yohannes and R. J. Doedens, *Angew. Chem., Int. Ed.*, 1999, **38**, 1292.

20 (a) S. S. Mal and U. Kortz, *Angew. Chem., Int. Ed.*, 2005, **44**, 3777; (b) S. S. Mal, B. S. Bassil, M. Ibrahim, S. Nellutla, J. V. Tol, N. S. Dalal, J. A. Fernández, X. López, J. M. Poblet, R. N. Biboum, B. Keita and U. Kortz, *Inorg. Chem.*, 2009, **48**, 11636.

21 J. Hua, Y. F. Qi, E. B. Wang, Y. G. Li, C. Qin, X. L. Wang and S. Chang, *Eur. J. Inorg. Chem.*, 2006, 4541.

22 (a) M. Hargittai, *Chem. Rev.*, 2000, **100**, 2233; (b) O. M. Yaghi and G. Li, *Angew. Chem., Int. Ed. Engl.*, 1995, **34**, 207; (c) P. M. Graham, R. D. Pike, M. Sabat, R. D. Bailey and W. T. Pennington, *Inorg. Chem.*, 2000, **39**, 5121; (d) G. H. Li, Z. Shi, X. M. Liu, Z. M. Dai and S. H. Feng, *Inorg. Chem.*, 2004, **43**, 6884; (e) A. J. Blake, N. R. Brooks, N. R. Champness, P. A. Cooke, M. Crew, A. M. Deveson, D. Fenske, D. H. Gregory, L. R. Hanton, P. Hubberstey and M. Schröder, *Chem. Commun.*, 2001, 1432; (f) J. J. M. Amoore, L. R. Hanton and M. D. Spicer, *Dalton Trans.*, 2003, 1056; (g) C. Näther and I. Jeb, *Eur. J. Inorg. Chem.*, 2004, 2868; (h) J. Y. Lu, B. R. Cabrera, R. J. Wang and J. Li, *Inorg. Chem.*, 1999, **38**, 4608; (i) Q. Hou, J. H. Yu, J. N. Xu, Q. F. Yang and J. Q. Xu, *CrystEngComm*, 2009, **11**, 2452.

23 J. P. Wang, P. T. Ma and J. Y. Niu, *Inorg. Chem. Commun.*, 2006, **9**, 1049.

24 N. E. Brese and M. O'Keefe, *Acta Crystallogr., Sect. B: Struct. Sci.*, 1991, **B47**, 192.